

## University of Southampton Research Repository ePrints Soton

Copyright © and Moral Rights for this thesis are retained by the author and/or other copyright owners. A copy can be downloaded for personal non-commercial research or study, without prior permission or charge. This thesis cannot be reproduced or quoted extensively from without first obtaining permission in writing from the copyright holder/s. The content must not be changed in any way or sold commercially in any format or medium without the formal permission of the copyright holders.

When referring to this work, full bibliographic details including the author, title, awarding institution and date of the thesis must be given e.g.

AUTHOR (year of submission) "Full thesis title", University of Southampton, name of the University School or Department, PhD Thesis, pagination

## Research Article

## Open Access

P. O'Mahoney\*, C. McDougall, P. Glynn-Jones, and M. P. MacDonald

# Acoustic trapping in bubble-bounded micro-cavities

DOI 10.1515/optof-2016-0003

Received September 23, 2016; revised October 24, 2016; accepted November 2, 2016

**Abstract:** We present a method for controllably producing longitudinal acoustic trapping sites inside microfluidic channels. Air bubbles are injected into a micro-capillary to create bubble-bounded 'micro-cavities'. A cavity mode is formed that shows controlled longitudinal acoustic trapping between the two air/water interfaces along with the levitation to the centre of the channel that one would expect from a lower order lateral mode. 7  $\mu\text{m}$  and 10  $\mu\text{m}$  microspheres are trapped at the discrete acoustic trapping sites in these micro-cavities. We show this for several lengths of micro-cavity.

**Keywords:** acoustic trapping; transducer; lab-on-a-chip; 3D trapping

## 1 Introduction

A core capability for most lab-on-a-chip and  $\mu\text{TAS}$  devices is the ability to manipulate particles or cells in small volumes, something which has been achieved through a wide variety of modalities and for applications such as single cell assays and cell sorting [1–3]. One of these modalities is acoustic trapping, which allows non-contact, parallelisable handling of objects from the micron scale upward [4, 5]. Particles are typically trapped and manipulated in standing wave patterns, with the interaction strength between the particles and the acoustic field depending on factors such as compressibility and density [6]. This provides a means of predictable non-contact localisation, which is particularly well suited to larger scale cell trapping and handling [7, 8].

Standing wave acoustic traps have found success in many different applications, such as cell sorting [9–12], patterning [13] and culture in suspension [14–16]. In order to achieve more localised or dextrous trapping, usually one must employ a more sophisticated transducer arrangement, for example changing the transducer shape and bonding points to form longitudinal modes in the capillary [17, 18], or by using a multi-element array to manipulate particles along a capillary [19]. While these methods have their own advantages, each serves to increase the complexity of the physical system in order to increase control.

Bubbles have been used previously in acoustic trapping methods. Rogers and Neild exploited the interplay of streaming and Bjerknes forces resulting from oscillating bubbles to selectively trap particles of different size and density [20]. The boundary walls of the bubbles can also be used to help create acoustic landscapes [21]. The use of bubbles increases the number of acoustically reflective surfaces, allowing for further means of shaping an applied acoustic field.

Micro-environments have also been devised previously in different modalities for many different applications, including acoustically levitated droplets for studying enzyme kinetics [22], using SAWs to create acoustic-counterflow and ultrafast microfluidics [23, 24], and high-throughput and low-reaction volume biology [25]. Some of these methods, however, are in open systems, and as such are potentially subject to contamination. Others are restricted by geometry and as such can lack reconfigurability and dexterity. A closed system in which control over particles or cells in a small volume is possible without contamination could be very useful in many biological applications, whilst maintaining adequate control over the particulate.

In this paper, we present a method for trapping particles with an ultrasonic standing wave in a small sample volume. Trapping using the acoustic standing wave in capillaries is usually restricted to by the geometry of the chamber in which acoustic resonance is achieved. However, using air bubbles injected into the flow as ultrasonic reflectors, one can produce customisable standing wave patterns to trap particles in a 3D array – vertically, hori-

**\*Corresponding Author: P. O'Mahoney:** Institute for Medical Science and Technology, University of Dundee, Dundee, DD2 1FD, UK, E-mail: pzomahoney@dundee.ac.uk

**C. McDougall, M. P. MacDonald:** Institute for Medical Science and Technology, University of Dundee, Dundee, DD2 1FD, UK

**P. Glynn-Jones:** Engineering Sciences, University of Southampton, Southampton, SO17 1BJ, UK



zontally and longitudinally - using a simple setup consisting of a glass capillary with a single transducer and driving frequency.

## 2 Experimental

### 2.1 Materials and methods

A common method of acoustic trapping is to use a half-wave resonance, in which a standing wave is formed between the walls of a channel [26]. Typically, fixing a transducer to one side of a capillary will render optical access impossible along that axis. However, the use of a transparent transducer means that optical access is preserved, allowing for observation through the transducer, and the potential for integration with optical manipulation systems [27]. For our chip fabrication, we use a disposable method similar to those used by Hammarström et al. [28].

To that end, a  $(300 \times 300) \mu\text{m}$  inner dimensions borosilicate glass capillary with  $150 \mu\text{m}$  wall thickness is fixed to a  $(1 \times 2) \text{cm}$  Lithium Niobate-Indium Tin Oxide (LNO-ITO) transducer. Lengths of  $0.8 \text{mm}$  I.D. Tygon tubing are connected to either end of the capillary to accommodate flow. A solution of  $7 \mu\text{m}$  and  $10 \mu\text{m}$  polymer microspheres is delivered via a syringe. A second syringe is inserted through the wall of the Tygon tubing, and is used to inject air bubbles into the flow. The fluid is pumped manually at a steady rate, with the air bubbles randomly injected in to the flow, thus creating different sized air-bounded fluid cavities in the tubing and capillary.

A simple microscope system is used to view the capillary, using Köehler illumination and a 5X long working distance objective (Mitutoyo, 378-802-6) with a CMOS camera (Point Grey, GS3-U3-23S6M-C). The fluid cavities are brought to rest in the viewing plane for observation.

The transducer is connected to the function generator with wires bonded by silver epoxy, and driven at  $4.34 \text{MHz}$ , which was experimentally found to produce a second harmonic acoustic resonance in the fluid cavity. Micro-cavities of various lengths are observed.

It is also of interest to show that the cavities can resonate at different harmonics, so to that end the response of the spheres in a micro-cavity are observed as the system is first driven at  $4.34 \text{MHz}$ , and then switched to  $2.15 \text{MHz}$ , which was found to give the fundamental mode across the channel walls.

## 2.2 Simulations

In order to gain insight into the acoustic field within the capillary, and verify that the boundary conditions supplied by the bubble were responsible for the observed pattern, a simplified model of our system was simulated using COMSOL 5. Figure 1 shows the modelled device.

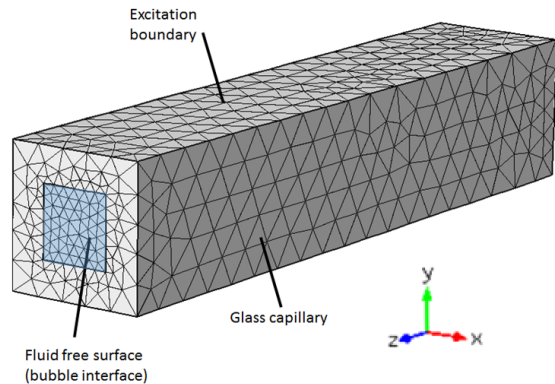


**Figure 1:** Finite element model of capillary. Acoustic resonances within the liquid filled core of the capillary are excited by an acceleration boundary condition on the top surface.

The model comprised linear elastic elements forming a square cross section glass capillary ( $300 \mu\text{m}$  inner dimensions, wall thickness  $150 \mu\text{m}$ ), and a “pressure acoustics” domain inside of it, representing the water. Rayleigh damping (corresponding to a Q-factor of 100) was added to the linear elastic elements to represent losses both within the material, and also into the support material. Previous work has found this to be a reasonable estimate [29], and the precise value is less important as we are more interested in mode shapes than their amplitudes. Mesh size was constrained to give a minimum of 6 elements across the width of the capillary. To reduce computational load, the transducer was not modelled explicitly, and the system was excited by a boundary stress on the lower face of the capillary. The curvature of the bubble interface was not modelled, and the cavity boundary represented by acoustic free surfaces that were flush with the ends of the  $3.20 \text{mm}$  modelled length. A range of excitation frequencies were simulated, and the results presented here are at the resonance where the energy density in the fluid reached a maximum which corresponds to the fundamental mode of the acoustic resonance in the modelled capillary.

### 3 Results and Discussion

We observed different lengths of micro-cavities showing various lateral harmonics as would normally be expected in an ultrasonic standing wave device. However, as a result of the introduction of bubbles into the capillary, it is clear (see Figure 2) that modes are being excited that create strong trapping nodes in the longitudinal direction in addition to the forces found acting in the square cross-section. The longitudinal part of the resonance is bounded by the air-water interfaces at either end of the fluid cavity. Using a simple cavity resonance model to predict the nodal spacing is found to be insufficient. Indeed, the resonance found at 4.34 MHz cannot be a simple  $\{2,2,n\}$  cavity resonance as this would be beyond the cut-off frequency for these cavity dimensions. Energy stored in the capillary walls and transducer thus plays an important role in defining the resonance. For the experimental results shown in Figure 2, using image analysis software (ImageJ), the distance ( $\pm$ SD) between the longitudinal nodes is measured to be  $143 \pm 5 \mu\text{m}$ .

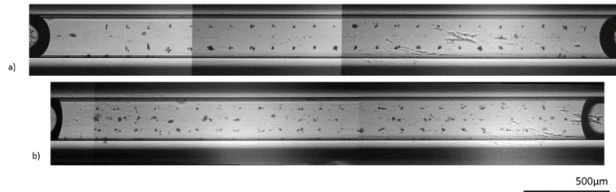


**Figure 2:** Acoustic trapping of  $7 \mu\text{m}$  and  $10 \mu\text{m}$  spheres in different sizes of micro-cavities. The micro-cavities have lengths (a)  $3.88 \text{ mm}$  and (b)  $3.72 \text{ mm}$ . The transducer is driven at  $4.34 \text{ MHz}$  in each case.

In Figure 3 we have shown the sequential excitation of two different harmonics in the same fluid cavity. The particles, initially held in the nodes created by driving the system at  $4.34 \text{ MHz}$ , migrate to the nodes present as the system is switched to a driving frequency of  $2.15 \text{ MHz}$ . This reaffirms some of our initial expectations with respect to the behaviour of the acoustic field in the micro-cavity, in that it has strong forces in the longitudinal,  $z$ , direction as well as in the other directions of the channel walls. The uniformity of the cavity mode wavelength in the longitudinal direction was not initially expected as the bubble boundary is neither a fixed nor a rigid surface like the channel walls, and we hypothesise that radiation forces on the bubble interface could be modifying the cavity length in a complex manner.

The modelling supports our interpretation of the trapping being caused by a resonant mode [30]. The model pre-

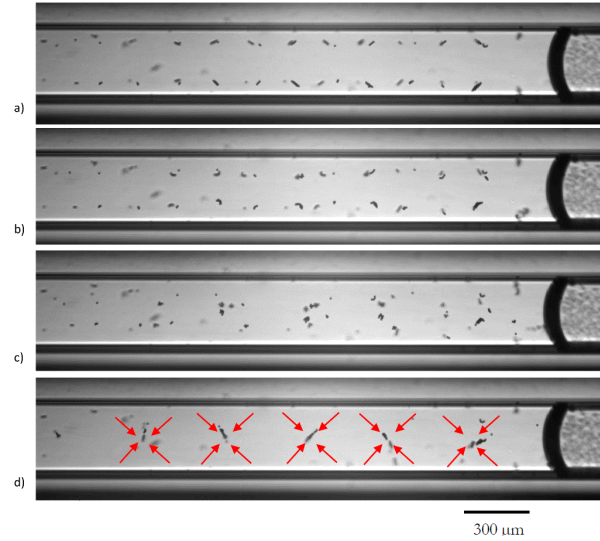


**Figure 3:** Resonant frequency of  $4.34 \text{ MHz}$  is applied (a), then the particle movement from (b), (c) to (d) when the function generator is instantaneously switched to  $2.15 \text{ MHz}$ . The red arrows in (d) indicate the direction the particles have travelled, from their initial to their final positions.

dicts a near uniform distribution of pressure along the  $x$ -direction, which is also observed in the motion of trapped particles in the experiments. Figure 4 shows the potential and kinetic energy densities corresponding to the pressure and velocity components of the acoustic field respectively. Assuming a particle with positive acoustic contrast factor, the Gor'kov equation [31] shows that particles experience forces attracting them to both the potential energy density minima, and the maxima of the kinetic energy density. The Gor'kov equation is shown in Equation 1 where  $V$  is the volume of the particle,  $\rho_p$  and  $\rho_f$  are the densities of the particle and fluid respectively, and  $c_p$  and  $c_f$  are the speeds of sound in the particle and surrounding fluid respectively [19].

$$\langle F \rangle = \nabla V \left( \frac{3(\rho_p - \rho_f)}{2\rho_p + \rho_f} \langle E_{kin} \rangle - \left( 1 - \frac{\rho_f c_f^2}{\rho_p c_p^2} \right) \langle E_{pot} \rangle \right) \quad (1)$$

The patterns obtained in Figure 4 correspond to the experimental results shown in Figure 3d. The effect of acoustic resonance between the bubble walls is clearly indicated by the periodic trapping along the channel length. The bubble walls are modelled as flat, solid boundaries in this instance, however in practice these surfaces are not fixed, and are free to move and deform. The difference in measured node spacing ( $\pm$ SD) between modelled and experimental values of  $356 \pm 6 \mu\text{m}$  and  $375 \pm 9 \mu\text{m}$  respectively is possibly due to the more complex excitation resulting from

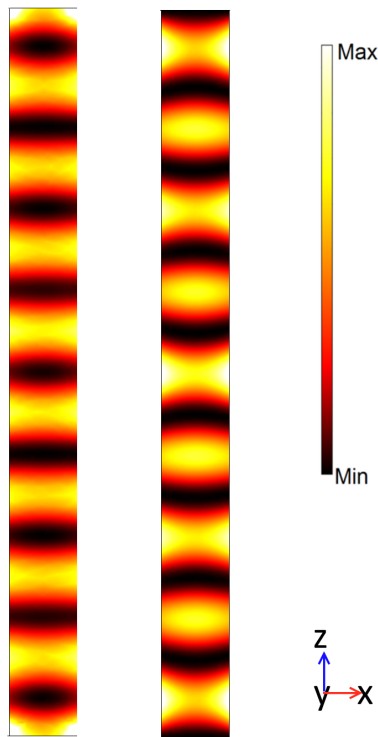


**Figure 4:** Normalised modelled energy densities (arbitrary units) on the central plane of the fluid cavity at a resonance of 1.97 MHz. Air bubbles are found at the top and bottom ( $\pm z$ ) boundaries of the figure. The particle trapping positions typically coincide at the minima of the potential energy density (left) and the maxima of the kinetic energy density (right). This is closely analogous to the experimental results in Figure 3(d).

the curved nature of the actual bubble surfaces and also due to non-modelled acoustic activity in the transducer.

Because the boundaries created by the bubbles are not fixed it is possible that the bubble walls may dynamically interact with the acoustic forces such that they can adjust to a lowest energy position for the system, removing the need for the bubbles to be precisely spaced in order to achieve a longitudinal resonance. This hypothesis was backed up by the fact that longitudinal resonances could be achieved in the presence of paired bubbles and lateral resonances even without controlling for the bubble spacing. Hence, bubbles introduced into an acoustic standing wave device give a robust and repeatable method for achieving strong longitudinal resonances for a range of frequencies.

## 4 Conclusions

Through the introduction of bubbles into simple microfluidic channels we have shown that it is possible to trap particles with significant trapping forces in three dimensional arrays of discrete acoustic nodes in small volumes of liquid. Our experiments and simulations confirm that it is possible to trap in the vertical, lateral and longitudinal directions simultaneously, using the channel walls in conjunction with air/water interfaces along the length of the channel. Three-dimensional localisation of particles in a small volume could find use in applications such as 3D cell patterning for parallelised micro-assays or encapsulation [32]. The use of a transparent transducer in this system allows for the addition of optical techniques, such as optical tweezers. Adding such a technique would further increase the dexterity of the system, and would open up the possibilities of single cell movement and force measurement/force calibration. The execution of these trapping geometries, combined with the very simple system, makes it an attractive consideration for future development. In particular, the intriguing possibility of a mechanism for the bubble boundaries to self-adjust to a resonance – in order to reach a lowest energy, equilibrium, position in the system – ensures that lateral and longitudinal resonances can be excited simultaneously without difficulty.

**Acknowledgement:** This work was supported by the SFC and an EPSRC Manufacturing with Light grant (EP/L022370/1).

Peter Glynne-Jones gratefully acknowledges support from EPSRC under Fellowship EP/L025035/1.

## References

- [1] J.-C. Baret, O. J. Miller, V. Taly, M. Ryckelynck, A. El-Harrak, L. Frenz, C. Rick, M. L. Samuels, J. B. Hutchison, J. J. Agresti, D. R. Link, D. a. Weitz, and A. D. Griffiths, “Fluorescence-activated droplet sorting (FADS): efficient microfluidic cell sorting based on enzymatic activity,” *Lab Chip*, vol. 9, no. 13, p. 1850, 2009.
- [2] J. F. Edd, D. Di Carlo, K. J. Humphry, S. Köster, D. Irimia, D. a Weitz, and M. Toner, “Controlled encapsulation of single-cells into monodisperse picolitre drops,” *Lab Chip*, vol. 8, no. 8, pp. 1262–1264, 2008.
- [3] J. Q. Boedicker, L. Li, T. R. Kline, and R. F. Ismagilov, “Detecting bacteria and determining their susceptibility to antibiotics by stochastic confinement in nanoliter droplets using plug-based microfluidics,” *Lab Chip*, vol. 8, no. 8, pp. 1265–1272, 2008.
- [4] L. King, “On the acoustic radiation pressure on spheres,” *Proc. R. Soc. Lond. A*, vol. 147, pp. 212–240, 1934.



- [5] B.-T. Chu, "Acoustic radiation pressure produced by a beam of sound," *J. Acoust. Soc. Am.*, vol. 72, p. 1673, 1982.
- [6] F. Petersson, L. Åberg, A. M. Swård-Nilsson, and T. Laurell, "Free flow acoustophoresis: Microfluidic-based mode of particle and cell separation," *Anal. Chem.*, vol. 79, no. 14, pp. 5117–5123, 2007.
- [7] T. Lilliehorn, U. Simu, M. Nilsson, M. Almqvist, T. Stepinski, T. Laurell, J. Nilsson, and S. Johansson, "Trapping of microparticles in the near field of an ultrasonic transducer," *Ultrasonics*, vol. 43, pp. 293–303, 2005.
- [8] D. Bazou, L. A. Kuznetsova, and W. T. Coakley, "Physical environment of 2-D animal cell aggregates formed in a short pathlength ultrasound standing wave trap," *Ultrasound Med. Biol.*, vol. 31, no. 3, pp. 423–430, 2005.
- [9] T. Franke, S. Braunmüller, L. Schmid, a Wixforth, and D. a Weitz, "Surface acoustic wave actuated cell sorting (SAWACS).," *Lab Chip*, vol. 10, no. 6, pp. 789–94, Mar. 2010.
- [10] X. Ding, S.-C. S. Lin, M. I. Lapsley, S. Li, X. Guo, C. Y. Chan, I.-K. Chiang, L. Wang, J. P. McCoy, and T. J. Huang, "Standing surface acoustic wave (SSAW) based multichannel cell sorting," *Lab Chip*, vol. 12, no. 21, pp. 4228–4231, 2012.
- [11] J. Dykes, A. Lenshof, I.-B. Åstrand-Grundström, T. Laurell, and S. Scheduling, "Efficient removal of platelets from peripheral blood progenitor cell products using a novel micro-chip based acoustophoretic platform.," *PLoS One*, vol. 6, no. 8, Jan. 2011.
- [12] T. Laurell, F. Petersson, and A. Nilsson, "Chip integrated strategies for acoustic separation and manipulation of cells and particles.," *Chem. Soc. Rev.*, vol. 36, no. 3, pp. 492–506, Mar. 2007.
- [13] J. Shi, D. Ahmed, X. Mao, S.-C. S. Lin, A. Lawit, and T. J. Huang, "Acoustic tweezers: patterning cells and microparticles using standing surface acoustic waves (SSAW)," *Lab Chip*, vol. 9, no. 20, pp. 2890–2895, 2009.
- [14] O. Doblhoff-Dier, T. Gaida, H. Katinger, W. Burger, M. Gröschl, and E. Benes, "A novel ultrasonic resonance field device for the retention of animal cells.," *Biotechnol. Prog.*, vol. 10, no. 4, pp. 428–32, 1994.
- [15] M. Gröschl, W. Burger, B. Handl, O. Doblhoff-Dier, T. Gaida, and C. Schmatz, "Ultrasonic Separation of Suspended Particles - Part III: Application in Biotechnology," *Acta Acust. united with Acust.*, vol. 84, no. 5, pp. 815–822, 1998.
- [16] L. R. Castilho and R. A. Medronho, "Cell retention devices for suspended-cell perfusion cultures," in *Tools and Applications of Biochemical Engineering Science*, Springer Berlin Heidelberg, 2002, pp. 129–169.
- [17] M. K. Araz and A. Lal, "Frequency Addressable Acoustic Collection, Separation and Mixing in a Pzt Driven Glass Capillary Microfluidic Actuator," in *14th International Conference on Miniaturized Systems for Chemistry and Life Sciences*, 2010, no. October, pp. 1919–1921.
- [18] O. Manneberg, S. Melker Hagsäter, J. Svennebring, H. M. Hertz, J. P. Kutter, H. Bruus, and M. Wiklund, "Spatial confinement of ultrasonic force fields in microfluidic channels," *Ultrasonics*, vol. 49, no. 1, pp. 112–119, 2009.
- [19] P. Glynne-Jones, C. E. M. Démoré, C. Ye, Y. Qiu, S. Cochran, and M. Hill, "Array-controlled ultrasonic manipulation of particles in planar acoustic resonator," *IEEE Trans. Ultrason. Ferroelectr. Freq. Control*, vol. 59, no. 6, pp. 1258–1266, 2012.
- [20] P. Rogers and A. Neild, "Selective particle trapping using an oscillating microbubble," *Lab Chip*, vol. 11, no. 21, pp. 3710–3715, 2011.
- [21] S. Oberti, A. Neild, R. Quach, and J. Dual, "The use of acoustic radiation forces to position particles within fluid droplets.," *Ultrasonics*, vol. 49, no. 1, pp. 47–52, Jan. 2009.
- [22] Z. N. Pierre, C. R. Field, and A. Scheeline, "Sample handling and chemical kinetics in an acoustically levitated drop microreactor," *Anal. Chem.*, vol. 81, no. 20, pp. 8496–8502, 2009.
- [23] M. Cecchini, S. Girardo, D. Pisignano, R. Cingolani, and F. Beltram, "Acoustic-counterflow microfluidics by surface acoustic waves," *Appl. Phys. Lett.*, vol. 92, no. 2008, 2008.
- [24] L. Y. Yeo and J. R. Friend, "Ultrafast microfluidics using surface acoustic waves," *Biomicrofluidics*, vol. 3, no. 2009, 2009.
- [25] V. Taly, B. T. Kelly, and A. D. Griffiths, "Droplets as microreactors for high-throughput biology," *ChemBioChem*, vol. 8, pp. 263–272, 2007.
- [26] A. Nilsson, F. Petersson, H. Jonsson, and T. Laurell, "Acoustic control of suspended particles in micro fluidic chips," *Lab Chip*, vol. 4, no. 2, pp. 131–135, 2004.
- [27] G. W. J. Brodie, Y. Qiu, S. Cochran, G. C. Spalding, and M. P. MacDonald, "Optically transparent piezoelectric transducer for ultrasonic particle manipulation.," *IEEE Trans. Ultrason. Ferroelectr. Freq. Control*, vol. 61, no. 3, pp. 389–91, Mar. 2014.
- [28] B. Hammarstrom, M. Evander, H. Barbeau, M. Bruzelius, J. Larson, T. Laurell, and J. Nilsson, "Non-contact acoustic cell trapping in disposable glass capillaries," *Lab Chip*, vol. 10, no. 17, pp. 2251–2257, 2010.
- [29] P. Glynne-Jones, R. J. Boltryk, and M. Hill, "Acoustofluidics 9: Modelling and applications of planar resonant devices for acoustic particle manipulation.," *Lab Chip*, vol. 12, no. 8, pp. 1417–26, Apr. 2012.
- [30] H. Bruus, "Acoustofluidics 2: perturbation theory and ultrasound resonance modes.," *Lab Chip*, vol. 12, no. 1, pp. 20–8, Jan. 2012.
- [31] L. Gor'kov, "On the forces acting on a small particle in an acoustical field in an ideal fluid," *Sov. Phys. Dokl.*, vol. 6, p. 773, 1962.
- [32] L. Gherardini, C. M. Cousins, J. J. Hawkes, J. Spengler, S. Radel, H. Lawler, B. Devcic-Kuhar, M. Gröschl, W. T. Coakley, and A. J. McLoughlin, "A new immobilisation method to arrange particles in a gel matrix by ultrasound standing waves," *Ultrasound Med. Biol.*, vol. 31, no. 2, pp. 261–272, Feb. 2005.